

---

1 **Effect and mechanism of perfluorooctanoic acid on extracellular polymeric substances of**  
2 **microorganisms during biological wastewater treatment**

3  
4 Jian Huang<sup>1,2,3</sup>, Xiaoyu Zheng<sup>1,2,3</sup>, Hua Zhang<sup>1,2,3\*</sup>, Tao Luo<sup>1,2,3</sup>, Jianye Cao<sup>4</sup>, Minli Lin<sup>4</sup>, Guowei  
5 Liu<sup>4</sup>, Zichen Shuai<sup>1,2,3</sup>

6 <sup>1</sup> School of Environmental and Energy Engineering, Anhui Jianzhu University, Hefei 230601, China

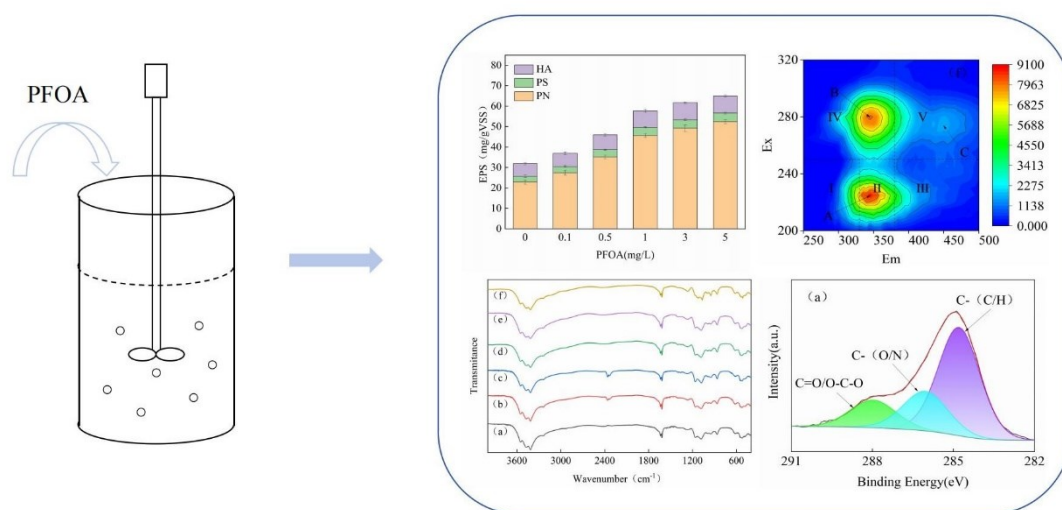
7 <sup>2</sup> Anhui Provincial Key Laboratory of Environmental Pollution Control and Resource Reuse, Hefei  
8 230601, China

9 <sup>3</sup> Pollution Control and Resource Utilization in Industrial Parks Joint Laboratory of Anhui Province,  
10 Hefei 230601, China

11 <sup>4</sup> Energy Conservation Renewable Energy Co., Ltd, Hefei, China

12  
13 \*Corresponding author:

14 E-mail: zhanghuapaper@163.com



16

17 **Abstract**

18 Perfluorooctanoic acid is ubiquitous in wastewater, bioaccumulative and biotoxic, and interferes with  
19 biological wastewater treatment. Extracellular polymeric substances are important components of  
20 microbial cells. The effects of perfluorooctanoic acid ( $0 \text{ mg L}^{-1}$ ,  $0.1 \text{ mg L}^{-1}$ ,  $0.5 \text{ mg L}^{-1}$ ,  $1.0 \text{ mg L}^{-1}$ ,  
21  $3.0 \text{ mg L}^{-1}$ , and  $5.0 \text{ mg L}^{-1}$ ) on extracellular polymeric substances were researched and the  
22 mechanisms were uncovered. The results indicated that the tightly bound extracellular polymeric  
23 substances (TB-EPS) initially increased and then decreased with the increase of perfluorooctanoic  
24 acid concentration, whereas the loosely bound extracellular polymeric substances (LB-EPS)  
25 consistently increased. Three-dimensional fluorescence spectroscopy revealed that the fluorescence  
26 intensity of TB-EPS components decreased, while that of LB-EPS components increased with the  
27 increase of perfluorooctanoic acid concentration. Fourier-transform infrared spectroscopy indicated  
28 the absorption peaks of functional groups, C=O, C-OH, C-O-C, C-N, or N-H in both TB-EPS and  
29 LB-EPS, shifted with the increase of perfluorooctanoic acid concentration. Protein secondary  
30 structure analysis demonstrated that perfluorooctanoic acid reduced the proportion of  $\alpha$ -helices,  
31 leading to loose protein structures. Additionally, X-ray photoelectron spectroscopy showed that, as

---

32 the concentration of perfluorooctanoic acid increased, the amount of C=O and O-C-O groups in LB-  
33 EPS increased and the proportion of C-(C/H) groups in TB-EPS decreased.

34 **Keywords:** Perfluorooctanoic acid, Biological wastewater treatment, Extracellular polymeric  
35 substances, Functional groups, Protein secondary structure

ACCEPTED MANUSCRIPT

---

## 36 1. Introduction

37 Perfluorooctanoic acid is widely used in textile, semiconductor, food packaging, and fire apparatus  
38 manufacturing industries(Forster et al., 2024). Current research has found that perfluorooctanoic acid  
39 is highly bioaccumulative and biotoxic, and prevalent in wastewater, drinking water(Sinkway et al.,  
40 2024), surface water(Zhu et al., 2024), sediment(T. Li et al., 2024), and soil(Lv et al., 2023). Studies  
41 have shown that perfluorooctanoic acid has an effect on biological wastewater treatment. Yu(X. Yu  
42 et al., 2018) et al. found that perfluorooctanoic acid inhibited the growth of microorganisms and  
43 affected the removal of dissolved organic carbon when perfluorooctanoic acid was 20 mg L<sup>-1</sup>. In the  
44 sequence batch reactor, perfluorooctanoic acid inhibited the activities of nitrate reductase, nitrite  
45 reductase, exophosphatase, polyphosphate kinase, and other major functional enzymes for  
46 denitrogenation and phosphorus removal, thus affecting the treatment effect of the reactor(X. Zheng  
47 et al., 2023). Li(W. Li et al., 2023) et al. demonstrated experimentally that the dewatering  
48 performance of sludge was significantly reduced when the concentration of perfluorooctanoic acid  
49 ranged from 1 mg L<sup>-1</sup> to 100 mg L<sup>-1</sup>. In addition, in the anammox system, perfluorooctanoic acid at  
50 concentrations ranging from 5 mg L<sup>-1</sup> to 50 mg L<sup>-1</sup> stimulated the production of reactive oxygen  
51 species in microorganisms and down-regulated the expression of genes involved in anammox and  
52 nitrification(Tang et al., 2022).

53 Extracellular polymeric substances in activated sludge play a crucial role in biological wastewater  
54 treatment(Y. Ma et al., 2023). Li(Z. Li et al., 2016) et al. showed that the flocculation of activated  
55 sludge is more effective and the average floc size is larger with the increase of extracellular polymeric  
56 substances. In addition, the research showed that the higher the ratio of extracellular proteins to  
57 extracellular polysaccharides, the better settling performance of the activated sludge. This is mainly  
58 due to the hydrophobicity of extracellular proteins(Yang et al., 2022). Additionally, various functional

---

59 groups in extracellular polymeric substances, such as hydroxyl, carboxyl, and amide groups, provide  
60 binding sites for the adsorption of organic and inorganic pollutants(Vandana et al., 2023). As a new  
61 pollutant, there are fewer studies related to the effects of perfluorooctanoic acid on microbial  
62 extracellular polymeric substances in biological wastewater treatment. Therefore, it is essential to  
63 study the effect and mechanism of perfluorooctanoic acid on extracellular polymeric substances to  
64 reveal the ecological hazards and mechanisms of perfluorooctanoic acid in biological wastewater  
65 treatment.

66 So this study aimed to investigate the effect of perfluorooctanoic acid on microbial extracellular  
67 polymeric substances in biological wastewater treatment and to reveal the effect mechanisms. First,  
68 the effects of different concentrations of perfluorooctanoic acid on the content and composition of  
69 microbial tightly bound extracellular polymeric substances (TB-EPS) and loosely bound extracellular  
70 polymeric substances (LB-EPS) were analyzed. Secondly, three-dimensional fluorescence  
71 spectroscopy and Fourier-transform infrared spectroscopy were used to study the effects of different  
72 concentrations of perfluorooctanoic acid on the composition and structure of extracellular polymeric  
73 substances. Finally, the potential effect mechanisms of perfluorooctanoic acid on the structure of  
74 extracellular polymeric substances was explored by protein secondary structure analysis, and X-ray  
75 photoelectron spectroscopy was used to determine the correlation between different concentrations  
76 of perfluorooctanoic acid and the proportion of functional groups in extracellular polymeric  
77 substances. This study provides further insight into the effects of new contaminants.

## 78 **2. Materials and methods**

### 79 *2.1 Experimental materials and design*

80 The perfluorooctanoic acid was purchased from Shanghai Aladdin Biotechnology Co. The stock  
81 solution of 1 g L<sup>-1</sup> perfluorooctanoic acid was configured by dissolving a gram of perfluorooctanoic

82 acid in a Liter of ultrapure water. The sludge used in the experiment was sourced from the aerobic  
83 end of a municipal wastewater treatment plant in Hefei, China. Synthetic wastewater was conducted  
84 in the experiment with CH<sub>3</sub>COONa, NH<sub>4</sub>Cl, and KH<sub>2</sub>PO<sub>4</sub>. The concentration of chemical oxygen  
85 demand (COD), ammonia nitrogen and soluble phosphorus was 150 mg L<sup>-1</sup>, 15 mg L<sup>-1</sup> and 6 mg L<sup>-1</sup>,  
86 respectively. The other compounds in the synthetic wastewater are listed in Table 1.

87  
88 **Table 1.** Content of trace elements in synthetic wastewater

ingredient	concentration (mg L <sup>-1</sup> )	ingredient	concentration (mg L <sup>-1</sup> )
Boric acid	0.10	Copper sulfate	0.03
Potassium iodide	0.18	Manganese chloride	0.12
Sodium Molybdate	0.06	Ferric chloride	1.50
Zinc sulfate	0.12	Cobalt chloride hexahydrate	0.08

89  
90 The six sequence batch reactors (SBRs) were utilized in the experiment. Each reactor operated for six  
91 cycles per day. Each cycle included a 15 minute influent period, a 60 minute anaerobic period, a 105  
92 minute aerobic period, a 40 minute settling period, a 15 minute effluent period, and a 5 minute idle  
93 period. The concentrations of perfluorooctanoic acid in each reactor were 0 mg L<sup>-1</sup>, 0.1 mg L<sup>-1</sup>, 0.5  
94 mg L<sup>-1</sup>, 1.0 mg L<sup>-1</sup>, 3.0 mg L<sup>-1</sup>, and 5.0 mg L<sup>-1</sup>, respectively. When these reactors were stable,  
95 perfluorooctanoic acid stock solution was added in each reactor. The extracellular polymeric  
96 substances were extracted for detection and analysis. All tests were conducted in triplicate from three  
97 parallel experiments, with values expressed as mean ± standard deviation.

## 98 *2.2 Extraction and content determination of extracellular polymeric substances*

99 Extraction of extracellular polymeric substances was conducted using thermal extraction as follows:

---

100 A 50 mL homogeneous sludge mixture was sampled from the aerobic end of the reactor. The sludge  
101 was washed three times with phosphate buffer, then centrifuged at 4°C and 4000 rpm for 5 minutes.  
102 The supernatant was removed. The phosphate buffer was preheated to 80°C and mixed with the  
103 remaining sludge for 1 min, then centrifuged at 4°C and 4000 rpm for 10 min. The supernatant was  
104 filtered using a 0.45 µm filter membrane to obtain the LB-EPS solution. The remaining sludge was  
105 resuspended in phosphate buffer, and heated in a water bath to 60°C. After 60 min, the mixture was  
106 centrifuged at 4°C and 4000 rpm for 15 min, and the supernatant was filtered using a 0.45 µm filter  
107 membrane to obtain the TB-EPS solution. Each extract was stored at 4°C for later use. The protein  
108 and humic acid content of extracellular polymeric substances were determined using the modified  
109 Lowry method(D. Ma et al., 2024), and the polysaccharide content was determined using the  
110 anthrone-sulfuric acid method(Peng et al., 2021).

### 111 *2.3 Three-dimensional fluorescence spectroscopy*

112 Three-dimensional fluorescence spectra of LB-EPS and TB-EPS samples were measured using a  
113 luminescence spectrometer. In the measurements, the excitation and emission wavelengths were set  
114 to 200-320 nm and 250-500 nm, respectively, and the scanning speed was 2400 nm min<sup>-1</sup>, using an  
115 excitation and emission interval of 10 nm. The data were processed using Origin 8.0 software.

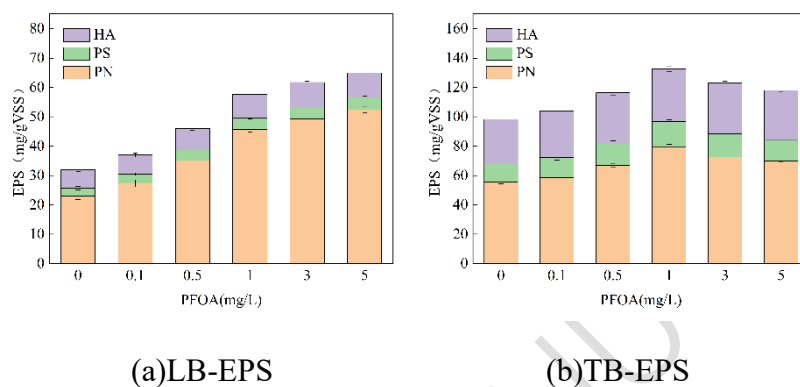
### 116 *2.4 Fourier-transform infrared spectroscopy and protein secondary structure analysis*

117 The Fourier-transform infrared spectroscopy of the LB-EPS and TB-EPS samples were measured  
118 using an FTIR instrument. In the measurement, the spectral range was set to 4000-400 cm<sup>-1</sup> with a  
119 resolution of 4 cm<sup>-1</sup>. The overlapping peaks in the amide I region were delineated using the  
120 deconvolution method through Peakfit software to obtain the proportion of protein secondary  
121 structure. The data were processed using Origin 8.0 software.

### 122 *2.5 X-ray photoelectron spectroscopy*

123 The C, O, and N elements in the extracellular polymeric substances were analyzed using X-ray  
124 photoelectron spectroscopy, and all binding energies were based on the neutral C 1s peak at 284.6 eV  
125 to compensate for surface charging effects. The X-ray photoelectron spectroscopy data were peak-  
126 split using Avantage software.

127



128 **Figure 1.** Changes of LB-EPS and TB-EPS under different concentrations of perfluorooctanoic acid

129

### 130 3. Results and analysis

#### 131 3.1 Effect of perfluorooctanoic acid extracellular polymeric substances

132 The changes in LB-EPS and TB-EPS components under different concentrations of perfluorooctanoic  
133 acid are showed in Figure 1. Figure 1 showed that low concentrations of perfluorooctanoic acid  
134 enhanced the secretion of extracellular polymeric substances in activated sludge. Conversely, high  
135 concentrations of perfluorooctanoic acid exhibit different effects on extracellular polymeric  
136 substances.

137 In Figure 1(a), the secretion of LB-EPS increases steadily with the increase of perfluorooctanoic acid  
138 concentrations. Specifically, when the perfluorooctanoic acid concentration was 5.0 mg L<sup>-1</sup>, the  
139 protein (PN), polysaccharide (PS), and humic acid (HA) contents in LB-EPS increased by 29.53 mg  
140 gVSS<sup>-1</sup>, 1.38 mg gVSS<sup>-1</sup>, and 2.19 mg gVSS<sup>-1</sup>, respectively, compared with the control group.

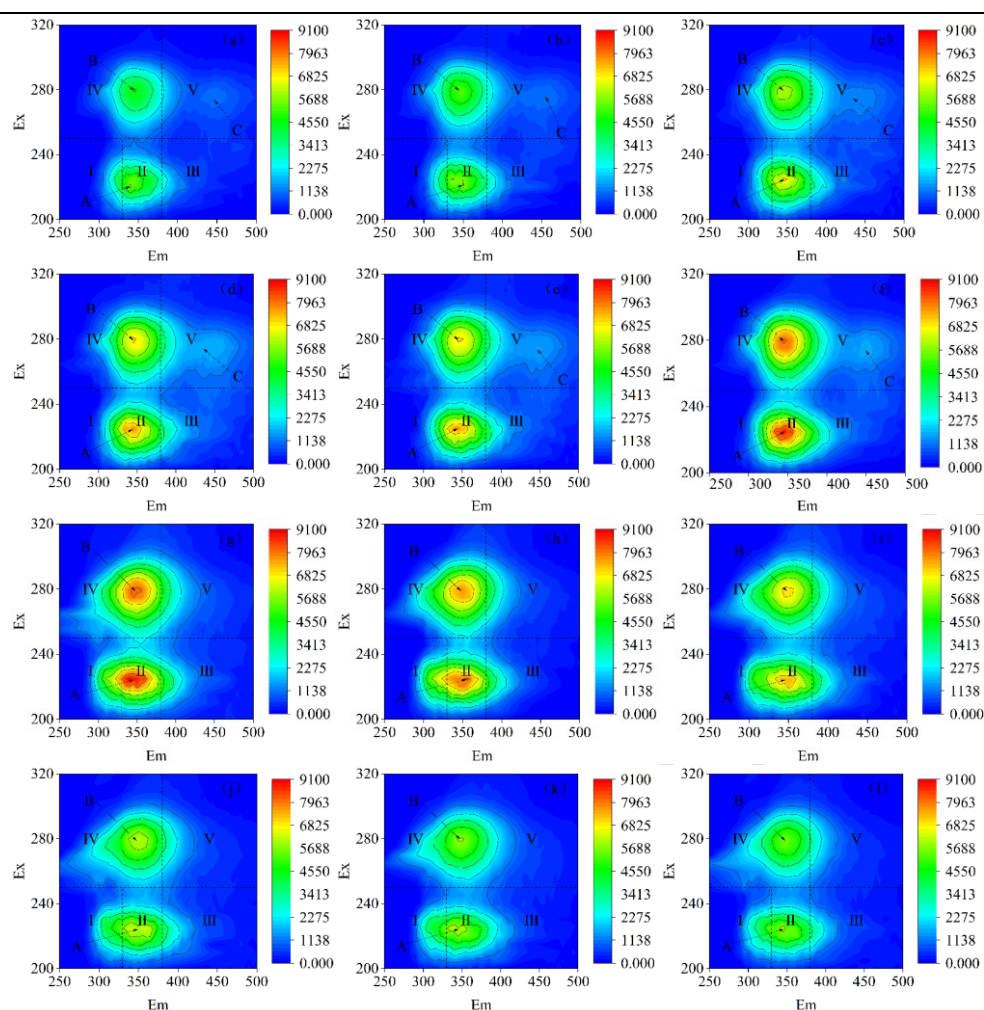


---

141 In Figure 1(b), In the control group, the content of PN, PS, and HA are 55.43 mg gVSS<sup>-1</sup>, 12.27 mg  
142 gVSS<sup>-1</sup>, and 30.52 mg gVSS<sup>-1</sup>, respectively. When the perfluorooctanoic acid concentration was 1.0  
143 mg L<sup>-1</sup>, the PN, PS, and HA contents increased to 79.55 mg gVSS<sup>-1</sup>, 17.24 mg gVSS<sup>-1</sup>, and 35.75 mg  
144 gVSS<sup>-1</sup>, respectively. Subsequently, As the concentration of perfluorooctanoic acid increased, the  
145 content of TB-EPS gradually decreased. Studies have shown that perfluorooctanoic acid a long-chain  
146 fluoride with strong hydrophobicity, readily binds to the internal structure of the phospholipid bilayer  
147 on cell membranes, leading to changes in cell membrane permeability(D. Li et al., 2023). Changes in  
148 the structure of the cell membrane will in turn disrupt the metabolism of the microorganisms,  
149 generating large amounts of reactive oxygen species that oxidize the fatty acids in the cell membrane,  
150 ultimately leading to cellular breakdown and inactivation of the microorganisms(T. Zheng et al.,  
151 2021). This may account for the reduced secretion of TB-EPS under high perfluorooctanoic acid  
152 conditions.

153 Under different concentrations of perfluorooctanoic acid concentration, PN accounted for 56%-81%  
154 of the sum of PN, PS and HA in LB-EPS and TB-EPS. Obviously, among the components of the  
155 extracellular polymers, the PN content accounted for the highest percentage. For example, when the  
156 perfluorooctanoic acid concentration was 5.0 mg L<sup>-1</sup>, the growth rates of PN, PS, and HA contents  
157 were 129%, 49%, and 36%, respectively, in LB-EPS, and the growth rates of PN, PS, and HA contents  
158 were 26%, 14%, and 11%, respectively, in TB-EPS. And the PN content was most significantly  
159 affected by perfluorooctanoic acid concentration. It has been shown that the changes in PN content  
160 are mainly related to the enzyme activities in microorganisms(Corsino et al., 2017). The  
161 perfluorooctanoic acid can reduce PN content by combining with enzymes to form aggregates,  
162 reducing enzyme activity and inhibiting their functioning(Xu et al., 2020).

163



164 **Figure 2.** Three-dimensional fluorescence spectroscopy of (a-f) LB-EPS and (g-l) TB-EPS at  
 165 different concentrations of perfluorooctanoic acid (where a-f and g-l characterize the concentrations  
 166 of perfluorooctanoic acid as 0 mg L<sup>-1</sup>, 0.1 mg L<sup>-1</sup>, 0.5 mg L<sup>-1</sup>, 1.0 mg L<sup>-1</sup>, 3.0 mg L<sup>-1</sup>, 5.0 mg L<sup>-1</sup>)

### 168 3.2 Effect of perfluorooctanoic acid on fluorescent compounds in extracellular polymeric substances

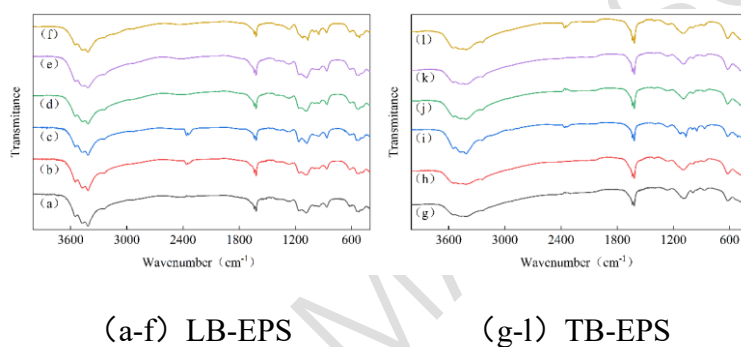
169 Figure 2 displays the three-dimensional fluorescence spectroscopy of LB-EPS and TB-EPS at  
 170 different concentrations of perfluorooctanoic acid. The spectrogram are segmented into five regions  
 171 based on excitation and emission wavelengths: fluorescent aromatic-like proteins I (200-250/250-330  
 172 nm), fluorescent aromatic-like proteins II (200-250/330-380 nm), fulvic acid-like substances (200-  
 173 250/380-500 nm), soluble microbial metabolites (250-320/250-380 nm), and humic acid-like  
 174 substances (250-320/380-500 nm). This study identified three prominent fluorescence peaks in

---

175 extracellular polymeric substances: Peak A (220-225/335-355 nm) for tryptophan-like substances,  
176 Peak B (280/345-350 nm) for soluble microbial products-like substances, and Peak C (270-275/435-  
177 455 nm) for humic acid-like substances(Qian et al., 2021).

178 When the concentration of perfluorooctanoic acid increased from 0 mg L<sup>-1</sup> to 5.0 mg L<sup>-1</sup>, the  
179 fluorescence intensities of peak A, peak B, and peakC in the spectra of LB-EPS increased from 5968,  
180 4642, and 1046 to 9016, 8091, and 1615, respectively. Conversely, the fluorescence intensities of  
181 peak A and peak B in the spectra of TB-EPS decreased from 9062 and 8057 to 6176 and 5435,  
182 respectively. The results indicate a significant increase in protein-like substances in LB-EPS with  
183 higher perfluorooctanoic acid concentrations, whereas the change in humic acid-like substances was  
184 more modest, consistent with the component analysis of LB-EPS. In TB-EPS, the fluorescence  
185 intensity of tryptophan-like substances and soluble microbial products-like substances decreased  
186 significantly with increasing concentrations of perfluorooctanoic acid. Analysis of TB-EPS  
187 composition suggests that the substantial fluorescence quenching observed in its spectra may be  
188 attributed to the higher binding affinity of its fluorescent organics for perfluorooctanoic acid.  
189 Guo(Guo et al., 2016) et al. demonstrated a prevalence of hydrophobic functional groups in TB-EPS  
190 compared to LB-EPS, facilitating binding with perfluorooctanoic acid. Regarding the position of  
191 fluorescence peaks, peak A, characteristic of tryptophan-like proteins in both LB-EPS and TB-EPS,  
192 exhibited a red-shift in the emission direction. This shift suggests an increase in carbonyl, carboxyl,  
193 and hydroxyl functional groups within the fluorescent moiety(Z. Liu et al., 2023), attributed to the  
194 presence of perfluorooctanoic acid. The experiment results also indicated that the binding of  
195 extracellular polymeric substances and perfluorooctanoic acid was closely related to the  
196 proteinaceous substances in the extracellular polymeric substances, mirroring the findings of Yan et  
197 al.(Yan et al., 2023).

198 Compared with TB-EPS, LB-EPS has a closer relationship with the dewatering performance of  
199 sludge(X. Y. Li & Yang, 2007); Liu(J. Liu et al., 2016) et al. showed that tryptophan and complex  
200 amino acids in sludge increase the difficulty of sludge-water separation, while humic acid has less  
201 effect on it. In addition, there are a large number of hydrophilic acids in the microbial metabolites,  
202 which will allow the extracellular polymers to fully absorb water. In conclusion, perfluorooctanoic  
203 acid promoted the secretion of tryptophan and microbial metabolites in LB-EPS, which adversely  
204 affected the sludge dewatering performance.



206 **Figure 3.** Fourier-transform infrared spectroscopy of LB-EPS and TB-EPS at different  
207 concentrations of perfluorooctanoic acid (where a-f and g-l characterize the concentrations of  
208 perfluorooctanoic acid as 0 mg L<sup>-1</sup>, 0.1 mg L<sup>-1</sup>, 0.5 mg L<sup>-1</sup>, 1.0 mg L<sup>-1</sup>, 3.0 mg L<sup>-1</sup>, 5.0 mg L<sup>-1</sup>)

### 209 3.3 Effects of perfluorooctanoic acid on functional groups and protein secondary structure in 210 extracellular polymeric substances

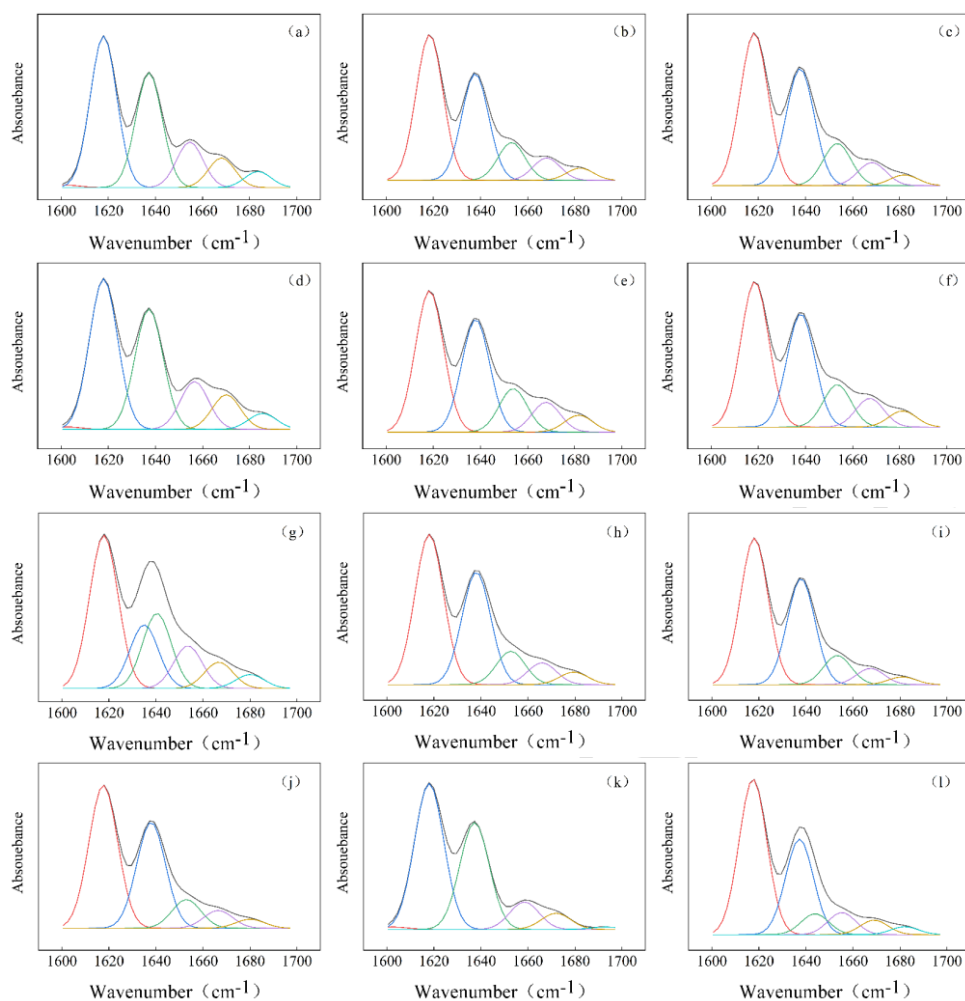
211 The effects of perfluorooctanoic acid on functional groups in extracellular polymeric substances are  
212 shown in Figure 3. As seen in Figure 3, Fourier-transform infrared spectroscopy can be divided into  
213 six regions: 1700 cm<sup>-1</sup>-1600 cm<sup>-1</sup> (amide I region), 1600 cm<sup>-1</sup>-1500 cm<sup>-1</sup> (amide II region), 1500 cm<sup>-1</sup>  
214 -1300 cm<sup>-1</sup> (carboxylic group-containing and hydrocarbon-like compounds), 1300 cm<sup>-1</sup>-1200 cm<sup>-1</sup>  
215 (amide III region), 1200 cm<sup>-1</sup>-900 cm<sup>-1</sup> (polysaccharides or nucleic acids), and 900-600 cm<sup>-1</sup>  
216

---

217 (fingerprint region)(Y. Li et al., 2023). The presence of absorption peaks in all regions indicates that  
218 the extracellular polymers have a complex composition.

219 In Fourier-transform infrared spectroscopy, the absorption peak near  $3413\text{ cm}^{-1}$  characterizes the  
220 stretching vibration of -OH; the absorption peak near  $1617\text{ cm}^{-1}$  belongs to the stretching vibration of  
221 C=C and C=O in the protein-associated amide I region; the absorption peak near  $1540\text{ cm}^{-1}$   
222 characterizes the stretching vibration of C-N and N-H in the protein-associated amide II region. The  
223 absorption peak near  $1400\text{ cm}^{-1}$  characterizes the C=O stretching vibration in the carboxyl group; the  
224 absorption peak near  $1263\text{ cm}^{-1}$  belongs to the C-N and N-H stretching vibration in the protein-  
225 associated amide III region; and the absorption peak near  $1159\text{ cm}^{-1}$  characterizes the C-OH stretching  
226 vibration in polysaccharides. The absorption peak near  $1081\text{ cm}^{-1}$  corresponds to the C-O-C stretching  
227 vibration in polysaccharides.

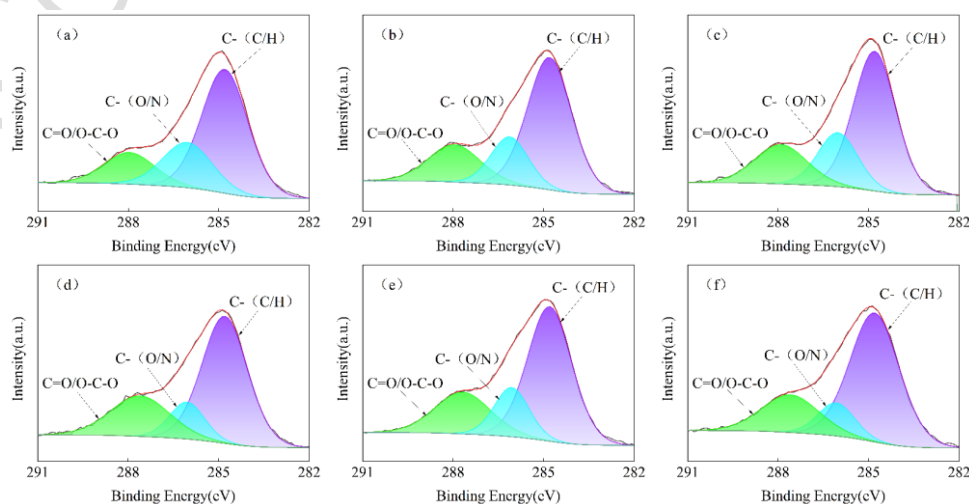
228 The shift in the positions of the absorption peaks in the spectra characterizes the structure change of  
229 the extracellular polymeric substances. With the increase of perfluorooctanoic acid concentrations,  
230 the positions of the absorption peaks at  $1400\text{ cm}^{-1}$ ,  $1263\text{ cm}^{-1}$ ,  $1159\text{ cm}^{-1}$ , and  $1081\text{ cm}^{-1}$  shift. The  
231 effects of perfluorooctanoic acid on functional groups in extracellular polymeric substances are  
232 mainly focused on carboxyl groups, protein-associated amide groups, and hydroxyl and ether bonds  
233 in polysaccharides. Yan et al.(Yan et al., 2021) concluded that the protonated amine in the amide  
234 group can interact electrostatically with the carboxyl head of perfluorooctanoic acid, facilitating its  
235 adsorption. Simultaneously, the hydroxyl group can form a hydrogen bond with the carboxyl head of  
236 the carboxyl group in perfluorooctanoic acid, stabilizing the hydrogen atom within an energy shell  
237 layer. These functional groups are also important constituents of enzymes in sludge, and their  
238 structural changes provide evidence for the previous speculation that perfluorooctanoic acid inhibits  
239 PN secretion by binding to related enzymes.

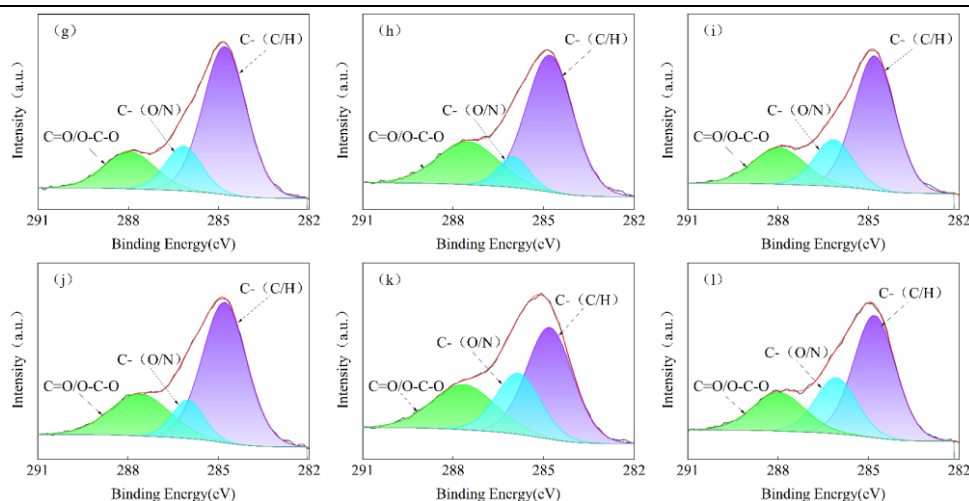


241 **Figure 4.** Fourier-transform infrared spectroscopy of (a-f) LB-EPS and (g-l) TB-EPS in the amide I  
 242 region (where a-f and g-l characterize the concentration of perfluorooctanoic acid as 0 mg L<sup>-1</sup>, 0.1  
 243 mg L<sup>-1</sup>, 0.5 mg L<sup>-1</sup>, 1.0 mg L<sup>-1</sup>, 3.0 mg L<sup>-1</sup>, 5.0 mg L<sup>-1</sup>)

244  
 245 The effects of different concentrations of perfluorooctanoic acid on the secondary structure of LB-  
 246 EPS and TB-EPS proteins in extracellular polymeric substances are shown in Figure 4. As seen in  
 247 Figure 4, the protein secondary structures are mainly categorized into four groups:  $\beta$ -sheet (1630 cm<sup>-1</sup>-  
 248 1640 cm<sup>-1</sup>), random coil (1640 cm<sup>-1</sup>-1650 cm<sup>-1</sup>),  $\alpha$ -helix (1650 cm<sup>-1</sup>-1660 cm<sup>-1</sup>), and antiparallel  $\beta$ -  
 249 sheet (1680 cm<sup>-1</sup>-1690 cm<sup>-1</sup>). When the concentration of perfluorooctanoic acid increased from 0 mg  
 250 L<sup>-1</sup> to 5.0 mg L<sup>-1</sup>, the  $\alpha$ -helix in LB-EPS and TB-EPS decreased from 13% and 11% to 12% and 7%,

251 respectively. In contrast, the  $\beta$ -sheets in LB-EPS and TB-EPS increased from 32% and 17% to 33%  
252 and 30%, respectively. The results indicated that perfluorooctanoic acid increased the proportion of  
253  $\beta$ -sheet structures and decreased the proportion of  $\alpha$ -helix structures in the amide I region of the  
254 protein. It has been demonstrated that perfluorooctanoic acid can alter proteins' secondary structure  
255 by reducing the energy required for  $\alpha$ -helix unfolding. Meanwhile, perfluorooctanoic acid binds to  
256 the unfolded body of the  $\alpha$ -helix through hydrogen bonding and hydrophobic interactions to form a  
257 more stable bound state(Yadav et al., 2024).  
258 It has been shown that the peptide bonds in each peptide chain can form hydrogen bonds, therefore,  
259 the  $\alpha$ -helix has high stability, while the  $\beta$ -fold is mainly formed by hydrogen bonds between carbonyl  
260 oxygen and amide hydrogen in the same or adjacent peptide chains(Wu et al., 2017).  $\alpha$ -helix/( $\beta$ -fold  
261 + irregular curls) is often used to characterize the compactness of the protein structure(E. Li et al.,  
262 2021). In this study, the proportion of  $\alpha$ -helix/( $\beta$ -folding + irregular curling) in LB-EPS and TB-EPS  
263 proteins was reduced from 40% and 31% to 37% and 18%, respectively, as the concentration of  
264 perfluorooctanoic acid increased. This result indicates that the structure of LB-EPS and TB-EPS  
265 became looser with increasing perfluorooctanoic acid concentration, which is unfavorable for sludge  
266 flocculation(J. Yu et al., 2023).





268 **Figure 5.** High-resolution C 1s spectra in the X-ray photoelectron spectroscopy of (a-f) LB-EPS  
 269 and (g-l) TB-EPS (where a-f vs. g-l characterize the concentration of perfluorooctanoic acid as 0 mg  
 270  $L^{-1}$ , 0.1 mg  $L^{-1}$ , 0.5 mg  $L^{-1}$ , 1.0 mg  $L^{-1}$ , 3.0 mg  $L^{-1}$ , 5.0 mg  $L^{-1}$ )

271

### 272 3.4 Effects of perfluorooctanoic acid on the elemental composition and functional groups of 273 extracellular polymeric substances

274 X-ray photoelectron spectroscopy was performed on the extracellular polymeric substances to further  
 275 investigate the effects of perfluorooctanoic acid on the elemental composition and characteristic  
 276 functional groups in LB-EPS and TB-EPS. The analytical results showed that the atomic ratios of  
 277 carbon (C) and oxygen (O) in the extracellular polymeric substances were 52%-57% and 37%-44%,  
 278 respectively, indicating high elemental abundances of C and O in LB-EPS and TB-EPS at various  
 279 concentrations of perfluorooctanoic acid. As the increase of perfluorooctanoic acid concentration, the  
 280 O/C molar ratios in LB-EPS and TB-EPS increased from 0.70 and 0.72 to 0.73 and 0.77, respectively.  
 281 Additionally, the N/C molar ratios increased from 0.10 and 0.12 to 0.12 and 0.14, respectively, when  
 282 the concentration of perfluorooctanoic acid was 5.0 mg  $L^{-1}$ . This suggested that perfluorooctanoic  
 283 acid promoted the secretion of nitrogenous and oxygenated compounds by microorganisms. Since  
 284 carbon (C 1s) is the central element in extracellular polymeric substances, this study further analyzes



---

285 high-resolution C 1s spectra to quantify each functional group as a molar ratio to the total carbon.  
286 This approach allows for comparisons of the various functional groups associated with carbon.  
287 The high-resolution C 1s spectra in the X-ray photoelectron spectroscopy of LB-EPS and TB-EPS  
288 are shown in Figure 5. As shown in Figure 5, three subpeaks can be decomposed from the C 1s peak:  
289 the C-(C/H) group near 284.8 eV, the C-(O/N) group near 286.3 eV, and the C=O or O-C-O group  
290 near 288.0 eV(An et al., 2023). When the concentration of perfluorooctanoic acid increased from 0  
291 mg L<sup>-1</sup> to mg L<sup>-1</sup>, the molar ratios of C=O or O-C-O in LB-EPS rose from 11.81% to 15.03%, while  
292 the molar ratio of C-(C/H) in TB-EPS decreased from 41.55% to 34.27%. The C-(C/H) groups are  
293 primarily derived from hydrocarbons, including the side chains of polysaccharides, amino acids, and  
294 lipids, and represent the main hydrophobic groups in extracellular polymeric substances. The less  
295 hydrophobic the extracellular polymer is, the higher the surface charge will be on the cell surface,  
296 which will be unfavorable for intercellular interactions. This will have an effect on the aggregation  
297 and stability of the activated sludge(Sun et al., 2024). The C=O or O-C-O groups are mainly present  
298 in extracellular polymers in the form of carboxylates, carbonyl groups, etc., which are negatively  
299 correlated with bioflocculation in wastewater biological treatment(Qian et al., 2021). The X-ray  
300 photoelectron spectroscopy analysis revealed that perfluorooctanoic acid changed the group  
301 occupancy of extracellular polymers, which adversely affected the flocculation and sedimentation  
302 effect and stability of activated sludge.

#### 303 **4. Conclusion**

304 The secretion of microbial extracellular polymers LB-EPS and TB-EPS was significantly promoted  
305 by low concentrations of perfluorooctanoic acid, but the promotion effect of TB-EPS secretion was  
306 weakened at higher concentrations of perfluorooctanoic acid. Perfluorooctanoic acid had different  
307 effects on the fluorescence intensity of LB-EPS and TB-EPS. With the increase of perfluorooctanoic

---

308 acid concentration, the intensity of microbial metabolite fluorescence peaks and tryptophan  
309 fluorescence peaks in TB-EPS decreased. However, the intensities of microbial metabolite  
310 fluorescence peaks, tryptophan fluorescence peaks and humic acid fluorescence peaks increased in  
311 LB-EPS, which implied that the dewatering performance of sludge became worse. Perfluorooctanoic  
312 acid affected the carboxyl groups, amide groups, ether bonds, and hydroxyl groups in the extracellular  
313 polymers, and the main binding modes of such functional groups to perfluorooctanoic acid included  
314 electrostatic interactions and hydrogen bonding. Perfluorooctanoic acid also affected the secondary  
315 structure of proteins in the extracellular polymers, decreasing the ratio of  $\alpha$ -helices/( $\beta$ -folds +  
316 irregular curls), which was detrimental to the settling performance of sludge. The relative content of  
317 C=O or O-C-O groups in LB-EPS increased with increasing concentrations of perfluorooctanoic acid,  
318 while the relative content of C-(C/H) groups in TB-EPS decreased, which had an effect on sludge  
319 stability. The experimental results show that the presence of perfluorooctanoic acid in wastewater  
320 should be given further attention. In addition, in order to fully describe the impact of  
321 perfluorooctanoic acid on biological wastewater treatment, the response of microbial communities  
322 and intracellular polymer substances to perfluorooctanoic acid needs to be further studied.

### 324 **Acknowledgments**

325 This work was supported by Anhui Provincial Key Research and Development Project  
326 (2023t07010002), Natural Science Research Project of Colleges of Anhui Province (KJ2021A0619),  
327 Cultivating academic (or disciplinary) leaders (DTR2023029), the National Natural Science  
328 Foundation of China (52300022), the Natural Science Foundation of Hefei (202310), Natural Science  
329 Research Project of Colleges of Anhui Province (2022AH050236, 2022AH010019).

- 332 Corsino, S. F., Capodici, M., Torregrossa, M., & Viviani, G. (2017). Physical properties and  
333 Extracellular Polymeric Substances pattern of aerobic granular sludge treating hypersaline  
334 wastewater. *Bioresource Technology*, 229, 152–159.
- 335 Forster, A. L. B., Geiger, T. C., Pansari, G. O., Justen, P. T., & Richardson, S. D. (2024). Identifying  
336 PFAS hotspots in surface waters of South Carolina using a new optimized total organic fluorine  
337 method and target LC-MS/MS. *Water Research*, 256, 121570.
- 338 Guo, X., Wang, X., & Liu, J. (2016). Composition analysis of fractions of extracellular polymeric  
339 substances from an activated sludge culture and identification of dominant forces affecting  
340 microbial aggregation. *Scientific Reports*, 6(1), 28391.
- 341 Li, D., Sun, C., Liu, X., Dai, Y., & Zhao, J. (2023). Interaction between per-and polyfluoroalkyl  
342 substances and microorganisms. *Chinese Science Bulletin*, 68(8), 872-885.
- 343 Li, E., Wang, Y., Zhang, D., Fan, X., Han, Z., & Yu, F. (2021). Siderite/PMS conditioning-pressurized  
344 vertical electro-osmotic dewatering process for activated sludge volume reduction: Evolution of  
345 protein secondary structure and typical amino acid in EPS. *Water Research*, 201, 117352.
- 346 Li, T., Chen, Y., Wang, Y., Tan, Y., Jiang, C., Yang, Y., & Zhang, Z. (2024). Occurrence, source  
347 apportionment and risk assessment of perfluorinated compounds in sediments from the longest  
348 river in Asia. *Journal of Hazardous Materials*, 467, 133608.
- 349 Li, W., Li, L., Li, B., Peng, L., Xu, Y., Li, R., & Song, K. (2023). Effect and mechanism of  
350 perfluorooctanoic acid (PFOA) on anaerobic digestion sludge dewaterability. *Chemosphere*, 335,  
351 139142.
- 352 Li, X. Y., & Yang, S. F. (2007). Influence of loosely bound extracellular polymeric substances (EPS)  
353 on the flocculation, sedimentation and dewaterability of activated sludge. *Water Research*, 41(5),  
354 1022–1030.
- 355 Li, Y., Fu, C., Cao, X., Wang, X., Wang, N., Zheng, M., Quan, L., Lv, J., & Guo, Z. (2023).  
356 Enhancement of sludge dewaterability by repeated inoculation of acidified sludge: Extracellular  
357 polymeric substances molecular structure and microbial community succession. *Chemosphere*,  
358 339, 139714.
- 359 Li, Z., Lu, P., Zhang, D., Chen, G., Zeng, S., & He, Q. (2016). Population balance modeling of  
360 activated sludge flocculation: Investigating the influence of Extracellular Polymeric Substances  
361 (EPS) content and zeta potential on flocculation dynamics. *Separation and Purification  
362 Technology*, 162, 91–100.
- 363 Liu, J., Wei, Y., Li, K., Tong, J., Wang, Y., & Jia, R. (2016). Microwave-acid pretreatment: A potential  
364 process for enhancing sludge dewaterability. *Water Research*, 90, 225–234.
- 365 Liu, Z., Yang, R., Zhang, D., Wang, J., Gao, M., Zhang, A., Liu, W., & Liu, Y. (2023). Insight into the  
366 effect of particulate organic matter on sludge granulation at the low organic load: Sludge  
367 characteristics, extracellular polymeric substances and microbial communities response.  
368 *Bioresource Technology*, 388, 129791.
- 369 Lv, L., Liu, B., Zhang, B., Yu, Y., Gao, L., & Ding, L. (2023). A systematic review on distribution,  
370 sources and sorption of perfluoroalkyl acids (PFAAs) in soil and their plant uptake.  
371 *Environmental Research*, 231, 116156.
- 372 Ma, D., Cheng, S., Zhang, Y., Ullah, F., Ji, G., & Li, A. (2024). Relation between  
373 hydrophilic/hydrophobic characteristics of sludge extracellular polymeric substances and sludge  
374 moisture-holding capacity in hot-pressing drying. *Science of The Total Environment*, 916,  
375 170233.

- 376 Ma, Y., Li, T.-Y., Meng, H., Wang, G.-X., Zhang, L.-M., Jia, G.-Z., Ma, J., Xiao, Y., Li, W.-H., & Xie,  
377 W.-M. (2023). The contradictory roles of tightly bound and loosely bound extracellular  
378 polymeric substances of activated sludge in trimethoprim adsorption process. *Journal of*  
379 *Environmental Management*, 336, 117661.
- 380 Peng, S., Hu, A., Ai, J., Zhang, W., & Wang, D. (2021). Changes in molecular structure of extracellular  
381 polymeric substances (EPS) with temperature in relation to sludge macro-physical properties.  
382 *Water Research*, 201, 117316.
- 383 Qian, J., He, X., Wang, P., Xu, B., Li, K., Lu, B., Jin, W., & Tang, S. (2021). Effects of polystyrene  
384 nanoplastics on extracellular polymeric substance composition of activated sludge: The role of  
385 surface functional groups. *Environmental Pollution*, 279, 116904.
- 386 Sinkway, T. D., Mehdi, Q., Griffin, E. K., Correia, K., Camacho, C. G., Aufmuth, J., Ilvento, C., &  
387 Bowden, J. A. (2024). Crowdsourcing citizens for statewide mapping of per- and  
388 polyfluoroalkyl substances (PFAS) in Florida drinking water. *Science of The Total Environment*,  
389 926, 171932.
- 390 Sun, S., Chen, Z., Wang, X., Wang, S., Liu, L., Yan, P., Chen, Y., Fang, F., & Guo, J. (2024). Effect  
391 of different feeding strategies on performance of aerobic granular sludge: From perspective of  
392 extracellular polymeric substances and microorganisms. *Journal of Environmental Chemical*  
393 *Engineering*, 12(1), 111688.
- 394 Tang, L., Su, C., Fan, C., Li, R., Wang, Y., Gao, S., & Chen, M. (2022). Long-term effect of  
395 perfluorooctanoic acid on the anammox system based on metagenomics: Performance, sludge  
396 characteristic and microbial community dynamic. *Bioresource Technology*, 351, 127002.
- 397 An, Q., Chen, Y., Tang, M., Zhao, B., Deng, S., Li, Z. (2023). The mechanism of extracellular  
398 polymeric substances in the formation of activated sludge flocs. *Colloids and Surfaces A:*  
399 *Physicochemical and Engineering Aspects*, 663, 131009.
- 400 Vandana, Priyadarshane, M., & Das, S. (2023). Bacterial extracellular polymeric substances:  
401 Biosynthesis and interaction with environmental pollutants. *Chemosphere*, 332, 138876.
- 402 Wu, B., Ni, B.-J., Horvat, K., Song, L., Chai, X., Dai, X., & Mahajan, D. (2017). Occurrence State  
403 and Molecular Structure Analysis of Extracellular Proteins with Implications on the  
404 Dewaterability of Waste-Activated Sludge. *Environmental Science & Technology*, 51(16),  
405 9235–9243.
- 406 Xu, M., Liu, G., Li, M., Huo, M., Zong, W., & Liu, R. (2020). Probing the Cell Apoptosis Pathway  
407 Induced by Perfluorooctanoic Acid and Perfluorooctane Sulfonate at the Subcellular and  
408 Molecular Levels. *Journal of Agricultural and Food Chemistry*, 68(2), 633–641.
- 409 Yadav, A., Vuković, L., & Narayan, M. (2024). An Atomic and Molecular Insight into How PFOA  
410 Reduces  $\alpha$ -Helicity, Compromises Substrate Binding, and Creates Binding Pockets in a Model  
411 Globular Protein. *Journal of the American Chemical Society*, 146(18), 12766–12777.
- 412 Yan, W., Qian, T., Zhang, L., Wang, L., & Zhou, Y. (2021). Interaction of perfluorooctanoic acid with  
413 extracellular polymeric substances—Role of protein. *Journal of Hazardous Materials*, 401,  
414 123381.
- 415 Yan, W., Song, M., & Zhou, Y. (2023). Redistribution of perfluorooctanoic acid in sludge after thermal  
416 hydrolysis: Location of protein plays a major role. *Water Research*, 241, 120135.
- 417 Yang, F., Huang, J., Xu, S., Huang, X., Guo, J., Fang, F., Chen, Y., & Yan, P. (2022). Influence of  
418 nitrogen-poor wastewater on activated sludge aggregation and settling: Sequential responses of  
419 extracellular proteins and exopolysaccharides. *Journal of Cleaner Production*, 359, 132160.
- 420 Yu, J., Xiao, K., Xu, H., Li, Y., Xue, Q., Xue, W., Zhang, A., Wen, X., Xu, G., & Huang, X. (2023).  
421 Spectroscopic fingerprints profiling the polysaccharide/protein/humic architecture of stratified

- 
- 422 extracellular polymeric substances (EPS) in activated sludge. *Water Research*, 235, 119866.
- 423 Yu, X., Nishimura, F., & Hidaka, T. (2018). Impact of Long-Term Perfluorooctanoic Acid (PFOA)
- 424 Exposure on Activated Sludge Process. *Water, Air, & Soil Pollution*, 229(4), 134.
- 425 Zheng, T., Li, J., & Liu, C. (2021). Improvement of  $\alpha$ -amylase to the metabolism adaptations of soil
- 426 bacteria against PFOS exposure. *Ecotoxicology and Environmental Safety*, 208, 111770.
- 427 Zheng, X., Zhang, H., Xu, Z., Lin, T., Yang, S., Zhao, Z., Han, Z., & Zhou, C. (2023). Tolerance and
- 428 recovery of aerobic granular sludge: Impact of perfluorooctanoic acid. *Chemosphere*, 313,
- 429 137430.
- 430 Zhu, X., Li, H., Luo, Y., Li, Y., Zhang, J., Wang, Z., Yang, W., & Li, R. (2024). Evaluation and
- 431 prediction of anthropogenic impacts on long-term multimedia fate and health risks of PFOS and
- 432 PFOA in the Elbe River Basin. *Water Research*, 257, 121675.

---

433 Dear Editor,

434 We have carefully revised the manuscript according to all suggestions made by the editor and the  
435 reviewers. We have carefully checked all author names and corrected exactly the style of the  
436 references and formatting according to the journal instructions. The revised manuscript looks much  
437 better than the original one, and we would like to take this opportunity to thank the editors for their  
438 valuable comments. We have included the e-mail addresses of all the co-authors at the end of this  
439 post

440  
441 Thank you for your time and consideration.

442  
443 Sincerely,

444  
445 Hua Zhang

446

447

448

449

450

451

452

453

454

455

---

456 **Response to editor and reviewers**

457 **Reviewer #A:**

458 I recommend acceptance of the manuscript after the authors successfully considered the reviewers  
459 comments.

460 Reply: Thank you for the valuable comments. We have made changes based on your comments.

461

462 **Reviewer #C:**

463 Your work has laid a solid foundation for future research, particularly in exploring the roles of ROS  
464 production, protein conformational changes, and enzymatic inhibition in microbial activity and  
465 extracellular polymer interactions. I encourage you to consider these factors in subsequent studies, as  
466 they could provide a more comprehensive understanding of how emerging contaminants affect  
467 microbial ecosystems in wastewater treatment.

468 Reply: Thank you for the valuable comments. Next, we will conduct further experiments to explore  
469 ROS generation, protein conformational changes and enzyme inhibition. Your suggestions allowed  
470 us to revise the manuscript in a reasonable way, so thank you again.

471

472

473

474

475

476

477

478

479

---

480 Co-author's e-mail  
481 Jian Huang:huangjianpaper@163.com;  
482 Xiaoyu Zheng:2459567346@qq.com;  
483 Hua Zhang: zhanghuapaper@163.com;  
484 Tao Luo:luotao\_edu@163.com;  
485 Jianye Cao:67863924@qq.com;  
486 Minli Lin:30592645@qq.com;  
487 Guowei Liu:117947453@qq.com;  
488 Zichen Shuai:3150381514@qq.com  
489

ACCEPTED MANUSCRIPT